buildings

MDPI

Review

Synergistically Using Bauxite Residue (Red Mud) and Other Solid Wastes to Manufacture Eco-Friendly Cementitious Materials

Lichao Feng [1], Wenliang Yao [1], Kai Zheng [2], Na Cui [3,*] and Ning Xie [2,*]

[1] School of Mechanical Engineering, Jiangsu Ocean University, Lianyungang 222005, China; lichaofeng@jou.edu.cn (L.F.); wenliangyao123@jou.edu.cn (W.Y.)
[2] Shandong Provincial Key Laboratory of Preparation and Measurement of Building Materials, University of Jinan, Jinan 250022, China; zhengkai1@ujn.edu.cn
[3] School of Civil Engineering and Architecture, University of Jinan, Jinan 250022, China
* Correspondence: cea_cuin@ujn.edu.cn (N.C.); mse_xien@ujn.edu.cn (N.X.); Tel.: +86-151-0531-1232 (N.C.)

Abstract: Bauxite residue (red mud) is a solid waste resulting from the aluminum production industry. Disposal or landfill of the red mud (RM) poses irreversible environmental problems; therefore, it is compelling to find practical solutions that can mitigate the negative environmental problems of RM stacking storage. In the past decades, although the recycling of RM has achieved significant progress, challenges remain from both academic and practical perspectives. Previous studies have demonstrated that all the aluminosilicate-based solid wastes have pozzolanic activity, and thus can be considered as resources to manufacture eco-friendly cementitious materials to relieve the carbon emission burden. Therefore, combining RM and other solid wastes to manufacture green cementitious materials has become a promising route to alleviate the burden of environmental pollutions. However, challenges from the fluctuation of the chemical compositions, inert activity, heavy metals stabilization, efflorescence, the side effects of the second pollutions from solid wastes, the hydration process, and mutual interaction mechanisms between the various types of solid wastes are still unclear, especially for multi-components RM-based cementitious materials. This review article summarizes the state of the art of mechanical properties, microstructure characterization methodologies, and hydration process and mechanisms of RM along with other solid wastes. The main challenges and future research trends are discussed. This article attempts to summarize the details of the RM recycling technologies that are beneficial to readers in understanding the background knowledge and research methodologies of eco-friendly cementitious materials.

Keywords: red mud; solid wastes; microstructure characterization; durability

Citation: Feng, L.; Yao, W.; Zheng, K.; Cui, N.; Xie, N. Synergistically Using Bauxite Residue (Red Mud) and Other Solid Wastes to Manufacture Eco-Friendly Cementitious Materials. *Buildings* **2022**, *12*, 117. https://doi.org/10.3390/buildings12020117

Academic Editors: Haoxin Li, Cong Ma and Tao Shi

Received: 23 November 2021
Accepted: 5 January 2022
Published: 25 January 2022

1. Introduction of Bauxite Residue (Red Mud)

Bauxite residue, also called red mud (RM), is the main solid waste in the aluminum production process. Currently, the annual disposal amount of RM has reached over 60 million tons, and over 1.3 billion tons in total are stacking in China, but with a recycling rate lower than 5% [1]. In Europe, dry stacking storage of RM was started about 50 years ago, and even at present, there are still many stacking storage places existing in Europe [2,3], and the negative effects of RM stacking have created significant environmental concerns.

As is well known, although the solubility of Al(III) in water is quite low, it keeps increasing with an increasing pH value. In the Bayer process, bauxite ore was mixed with a sodium hydroxide solution in a pressure vessel at 150 to 200 °C to extract sodium aluminate $[Al(OH)_4]^-$. As a result, the bauxite residue (red mud) was a high pH value material due to the high concentrations of calcium and sodium hydroxide along with a complex chemical composition, and it has become one of the main solid wastes that pose significant environmental problems. Although RM has been considered as solid

waste, from the perspective of materials chemistry, it is a promising raw material for manufacturing cementitious materials due to the fact that the main chemical compositions of RM are primarily composed of iron oxides (5–30%), titanium dioxide (2–15%), calcium oxide (0–20%), silicon oxide (5–50%), and undissolved alumina (0–20%) [4,5], which ensure the potential pozzolanic activity of the RM. A previous study found that the replacement of RM in ordinary Portland cement could reduce the total porosity of 7 d mortar samples compared with the controlled cement samples, although the total porosity of the 90 d samples with a 20% RM replacement was slightly higher than controlled cement and cement/fly ash samples. For the pore size distribution, it was claimed that the replacement of RM in cement could increase the volume of the pores with sizes smaller than 100 nm due to the pozzolanic activity of the RM and the filling effect of the fine RM particles [6].

Despite RM having a similar chemical composition to aluminosilicate and showing a potential pozzolanic activity, its inert nature has significantly confined its application to cementitious material directly. In the 1980s, through an alkali-activating method, Prof. Joseph Davidovits issued his patent by inventing a high-strength cementitious binder, named "geopolymer" [7]. From then on, the related research of aluminosilicate cementitious materials has developed rapidly. It was demonstrated that the hydration products of ancient architecture are stable zeolite-like phases [8–10], and other studies have also claimed that the hydration products of metakaolin-based aluminosilicate are gradually transformed from C-S-H, C-A-S-H, and N-A-S-H to a stable zeolite structure [11]. For the aluminosilicate, it was found that the hydration degree is governed by the molar ratio and alkali content of the activator. It was pointed out that silica tetrahedral monomers, which were beneficial to the formation of a final hydration product gel phase, could be formed by using water glass as the activator [12]. Previous studies have claimed that the activation process of aluminosilicate is mainly divided into two steps, namely, the bond-breaking process and the bond re-organizing process of Ca-O, Si-O-Si, Al-O-Al, and Al-O-Si in raw materials [13].

Although previous studies have demonstrated that RM can be used in manufacturing Portland cement and calcium sulfoaluminate cement, such as for supplementary cementitious materials in blended cement measuring about 1.5 million tons [14,15], as building materials such as bricks and tiles (about 300,000 tons), and as landfill/roads/soil amelioration (about 500,000 tons) [16], most RM is dry stacked in various areas, and over 90% is not recycled. In 2020, the International Aluminum Institute launched a Roadmap for maximizing the use of RM in cement, in which details on how to recycle the RM cement production and knowledge gaps and barriers, including soluble sodium, activation, and leaching problems, were summarized [17].

In the past decade, the exploration of up-cycling use of solid waste as raw materials to manufacture eco-friendly cementitious materials has attracted extensive interest worldwide due to the huge environmental burden resulting from the stacking and landfill of these solid wastes [18–20]. Previous studies have demonstrated that synergistically using various solid wastes is a promising approach to mitigating the challenges of the fluctuation of the chemical compositions, non-activity, heavy metals immobilization, and the side effects of secondary pollutions from solid wastes; however, the hydration process and mutual interaction mechanisms between the various types of solid wastes are still unclear, especially for multi-component RM-based cementitious materials. Although several outstanding review articles have extensively summarized the research gaps and challenges of RM recycling technologies [21–24], including how to combine RM and other solid wastes to manufacture eco-friendly cementitious materials, what is the optimized mixture proportion, what are the main hydration products, what are the mutual interaction mechanisms, and what are the practical application protocols, were barely systematically discussed. According to these challenges, in this review article, how RM was up-cycled by combining it with other solid wastes, including lime, coal gangue, metakaolin, slags, fly ash, and husk ashes, is reviewed, and the interaction mechanisms and influencing factors are summarized in the following sections (*Although the sections are divided by using the types of solid wastes as the sub-headings, they are not limited to binary systems*). This article is not only beneficial

for understanding the hydration mechanism of RM combined with other solid wastes when preparing eco-friendly cementitious materials, but it is also a guideline for potential practical applications in low-carbon constructions.

2. Lime

Lime is a calcium-containing mineral mainly composed of calcium oxide and calcium hydroxide. The alkali nature of lime is beneficial for activating the aluminosilicate contents in RM to form a cementitious binder phase, such a C-S-H or C-A-S-H which contributes to the mechanical strength of the material. In the early 1990s, the mechanical properties of RM/lime bricks were investigated in India. It was found that with a 5% lime addition, the maximum 28 days compressive strength can reach 3.75 MPa, and with an 8% lime addition, the maximum 28 days compressive strength can reach 4.22 MPa, provided there are humid curing conditions. In this study, the chemical compositions of RM were SiO_2 (6–10%), Al_2O_3 (19–26%), Fe_2O_3 (23–31%), TiO_2 (20–27%), CaO (2–4%), K_2O/Na_2O (4–7%), and LOI (8–11%). The lime was a fully hydrated class C lime and although the authors did not implement any microstructure analysis, they still provided a few potential mechanisms that might explain the RM hydration. First, lime is beneficial for forming large size aggregates with the flocculation of fine RM particles; second, the carbonation of lime forms $CaCO_3$ which provides the cementing action; and third, the pozzolanic reaction of lime with the RM generates new hydration products due to the preferential absorption of Ca cations rather than the alkali cations on the RM particles [25].

In 1996, a Jamaica-based research group further investigated the strength development of the RM/lime system. The main composition of the RM in this study was SiO_2 (3–8%), TiO_2 (6–7%), Al_2O_3 (16.5%), Fe_2O_3 (43–50%), CaO (6–9%), K_2O/Na_2O (2–5%), and LOI (10–12 %). The main difference in chemical composition between these two studies resides with the TiO_2 and Fe_2O_3. This study had two additional steps than Arjun's work. First, the mechanical properties were significantly enhanced. The 28 days compressive strength reached 15–18 MPa, and 122 days compressive strength reached 18–22 MPa and apart from the mechanical properties, this study moved a big step forward on the microstructure characterization. XRD, DTG, and SEM were used to characterize the hydration products. The XRD results indicated that the strength enhancement was mainly associated with the formation of stratlingite (C_2ASH_8) and carbonates. One thing to be noted here is that a small amount of silica fume was mixed with the RM/lime system, and the ratio of the lime and silica fume was 2:1 to form the calcium silicate phase [26].

After twenty years of development, although the mechanical properties were not palpably improved, the understanding of the RM/lime system has made considerable progress. Mymrin's study demonstrated that once mixed with lime waste and furnace slag, the 3, 7, 14, and 365 days compressive strengths of RM were 1.8, 3.4, 6.2, and 11.2 MPa, respectively. In this study, the chemical compositions of the RM were SiO_2 (11.7%), TiO_2 (15.2%), Al_2O_3 (12.6%), Fe_2O_3 (35.5%), CaO (14.8%), Na_2O (4.6%), and MgO (1.1%). The lime waste was composed of SiO_2 (0.7%), MgO (28.3%), CaO (45.1%), Al_2O_3 (1.1%), and Fe_2O_3 (0.9%). In this RM/furnace slag system, although the amount of the lime waste was only about 3%, the compressive strength showed a sharp increase of over 50% higher than the non-lime addition samples. Unfortunately, the reaction mechanism of the lime was NOT deeply elucidated although the authors had tested the XRD and SEM of the hydrated samples [27].

A recent study reported the mechanical properties of RM/lime systems incorporated with fly ash. The RM in this study was obtained from two locations, and the chemical compositions had a slight difference. The chemical compositions of the RM received from the Shandong aluminum industry Co., Ltd. were Na_2O (6.21%), Al_2O_3 (17.37%), SiO_2 (14.03%), SO_3 (0.45%), CaO (9.56%), TiO_2 (4.87%), and Fe_2O_3 (24.87%), and the RM received from the Weiqiao pioneering group Co., Ltd. were Na_2O (5.84%), Al_2O_3 (22.25%), SiO_2 (10.78%), SO_3 (0.91%), CaO (2.90%), TiO_2 (4.91%), and Fe_2O_3 (33.16%). In addition, the effective CaO and MgO contents in the lime were about 55%. The proportion of RM was

varied from 17.5% to 75%, and the lime contents were varied from 2.3% to 45%, with fly ash and soil used as the balance. In this study, the ratio between the lime and fly ash was used as a parameter to test the effect on the mechanical properties. The results indicated that the best proportion of this system should be 50% of lime and fly ash with a ratio of 3:2, 35% RM, and 15% soil. After being cured at room temperature with a relative humidity of 95%, the optimized 7 d and 28 d unconfined compressive strengths were 1.8 and 2.3 MPa, respectively. Via XRD and SEM/EDS analysis, the authors concluded that the main early strength was originated from the formation of $Ca_3Al_2O_6$, and the boehmite (c-AlO(OH)) and goethite (FeO(OH)) were the active components in the RM that reacted with the lime and fly ash. Furthermore, the late stage strength was originated from the formation of C-S-H and $CaAl_2Si_2O_8 \cdot 4H_2O$ phases [28].

Several impact factors on the mechanical properties were presented, including water content, lime content, dry density, molding water/lime ratio, porosity/volumetric lime content, and microstructure. It was concluded that the unconfined compressive strength increased non-linearly with an increasing lime content from the dry density perspective. For the impact of the water/lime ratio, the reduction of this value was beneficial to enhance the mechanical properties, and it followed a power function. In addition, the decrease of porosity/volumetric lime content ratio had a positive effect on strength enhancement, but no quantitative relationship could be obtained. The authors gave an empirical equation to calculate the unconfined compressive strength of the RM/lime cementitious materials including the above-mentioned factors, shown as:

$$Q = 4.93E + 11[\eta/(L_v)^{0.11}]^{-5.11} \quad (1)$$

where Q is the unconfined compressive strength, η is the porosity, and L_v is the volumetric lime content [29].

Apart from contributing to the mechanical properties, the addition of lime in RM has an important positive effect on immobilizing the heavy metals and soluble ions when considering the environmental concern of solid wastes' recycling. Although Garau's study was not focused on investigating the RM/lime system for manufacturing cementitious materials, they did shed a light on the possibility of immobilizing heavy metals by using the RM/lime system with zeolite as additives in polluted soils. The results indicated that the soluble Pb, Cd, and Zn contents could be reduced in acidic soil; however, due to the main purpose of this study was not the investigation of cementitious materials, the interaction mechanisms between the RM and lime were not discussed [30]. Similar studies have also demonstrated that the heavy metals in soils can be immobilized by using RM along with lime [31,32].

Based on the studies in soils, in this decade, researchers have started to explore the feasibility of using lime to improve heavy metal immobilization in RM-based cementitious materials. In an RM and Pb/Zn smelter waste system that contained arsenic and heavy metals, the RM showed observable potential cementitious characteristics. The leaching and toxicity testing results demonstrated that the concentrations of heavy metals were significantly dependent on the chemical speciation of arsenic and the hydration products. In this RM/sludge waste system, the aluminum oxide could be activated by lime effectively to form hydration products. For example, some aluminum positions in the ettringite lattice could be replaced by iron to form calcium sulfoferrite hydration products. The 28 day compressive strength reached 12.05 MPa, and the concentration of As was 0.6 mg/L. It was claimed that this system meets the requirements from the China Standard of Leaching Test and, therefore, can be used as an eco-friendly cementitious material [33].

A most recent study investigated the leaching of Cu, Pb, and Zn in an RM-based cementitious binder by using lime as a key element to improve the heavy metals immobilization ability of the RM binder. It was found that the leachate concentrations of Cu, Pb, and Zn from the RM binder decreased significantly with the increase of lime content. The leachate concentrations, with values of Cu (100 mg/L), Zn (100 mg/L), and Pb (5 mg/L), satisfy the requirements of the Ministry of Environmental Protection and the requirements

of GB5083-2007. According to the microstructure analysis, it was concluded that the heavy metals enter the ettringite lattice resulting in chemical trapping. The SEM image shows that in the RM cementitious binder phase, the unreacted hematite presents in the form of large particles, and with an increasing CaO content and pH value, the particle size of the ettringite reduced and attached to the surface of the large hematite particles which is beneficial for heavy metal fixing on the particles. When heavy metals are fixed on the surface of the particles, the SO_4^{2-} in the ettringite phase is replaced by other acid ions in the solution. Although this study gives a potential heavy metal immobilization mechanism for the lime in RM, it was not enough to directly prove this assumption based on the SEM and TGA results alone [34].

Although it has been widely accepted that the addition of lime is beneficial to enhance the mechanical properties of RM-based cementitious materials due to the ability of lime activating the aluminum oxide and silica in RM, the conflict between the early age strength and workability is still the main practical challenge. In addition, although current research has used a few microstructure characterization methods, the real enhancement mechanism of the mechanical properties is still unknown, especially concerning the early age strength. The hydration products, microstructure evolution process, and the reaction rates of the diverse phases remain unclear. Furthermore, it has been proved that lime has a positive effect on heavy metals immobilization, and while the potential mechanism has been presented, agreement has not yet been achieved. Therefore, it is essential to elucidate the mechanical enhancement mechanism through a quantitative advanced microstructure analysis, thus, helping to design a RM eco-friendly cementitious materials system.

3. Coal Gangue

Coal gangue is a solid waste that is produced during the mining and washing of coal. Due to coal being the largest energy resource, the accumulative amount of coal gangue has reached approximately three billion tons in China and keeps increasing annually along with coal mining activities. It has become one of the largest industrial solid wastes that needs to be dealt with. Due to the main chemical compositions of the coal gangue being SiO_2 (52–65%), Al_2O_3 (16–36%), Fe_2O_3 (2.28–14.63%), K_2O/Na_2O (1.45–3.9%), CaO (0.42–2.32%), MgO (0.44–2.41%), TiO_2 (0.90–4%), and P_2O_5 (0.007~0.24%), it is feasible to recycle the coal gangue as a potential resource for manufacturing cementitious materials.

In 2009, Zhang et al. explored the possibility of incorporating RM and coal gangue to manufacture eco-friendly cementitious materials. The authors defined the RM/coal gangue mixture as a "silica/alumina-based cementitious material". The RM and coal gangue with a ratio of 3:2 were homogeneously mixed with a water/solid ratio of 0.3. The mixture was calcined at 600 °C for 2 h followed by being air-cooled and ball milled to a powder, then subsequently the calcined mixture (50%) was blended with blast furnace slag (24%), clinker (20%), and gypsum (6%). In this study, the chemical compositions of RM were SiO_2 (17.78%), Al_2O_3 (6.27%), CaO (37.52%), Fe_2O_3 (12.32%), K_2O/Na_2O (3.21%), MgO (1.15%), TiO_2 (3.27%), SO_3 (0.49%), and loss of ignition (17.76%). Meanwhile, the chemical compositions of the coal gangue were SiO_2 (49.41%), Al_2O_3 (21.32%), CaO (2.52%), Fe_2O_3 (6.02%), K_2O/Na_2O (4.29%), MgO (1.56%), TiO_2 (0.94%), SO_3 (0.65%), and loss of ignition (12.75%). The slag and the clinker were mainly composed of SiO_2, Al_2O_3, CaO, Fe_2O_3, and MgO. Through the microstructure analysis, it was found that the main hydration products of the RM/coal gangue system were ettringite, calcium hydroxide, and C-S-H binder phase, in which the C-S-H phase and the ettringite contributed the mechanical properties at the early age. The SEM morphologies of the 28 day and 90 day samples demonstrated a dense amorphous C-S-H layer on the non-reacted RM and coal gangue particles. The EDS results indicated that part of the C-S-H phase had changed into a N-A-S-H structure with an increasing hydration age. The authors also agreed that further investigation was necessary to explain this phenomenon [35].

Based on this assumption, two years later, the authors systematically investigated the microstructure development of the RM/coal gangue system with the presence of

lime. Before the lime was mixed with the RM/coal gangue system, the raw materials and the preparation procedure were the same as in their previous study. The dosage of the lime was 10%, 15%, and 20%, and the XRD, FTIR, and TG/DTA were combined to investigate the microstructure development procedure. It was claimed that the hydration products were mainly the aluminous C-S-H and $Ca_3Al_2O_6 \cdot xH_2O$. The TG results indicated that the high amount of Ca $(OH)_2$ in the pastes was not conducive to the continuous increase of non-evaporable water content. A big step forward of this study was that the authors used the ^{27}Al MAS NMR to investigate the coordination state of the Al in the hydration product phases. The results indicate that the content of $Al^{[4]}$ in the C-A-S-H phase remained relatively constant during the hydration progress, while the content of $Al^{[6]}$ in $Ca_3Al_2O_6 \cdot xH_2O$ increased significantly with the elongation of the hydration time. Although this study shed a light on the role of the Al in the RM/coal gangue system, the lack of Si analysis caused the unclear Al-Si-O structural description [36]. Similar XRD, FTIR, and TG/DTA testing results were implemented to further confirm the hydration process of the RM/coal gangue system [37,38].

To further understand the structure of Al, Si, and O in an RM/coal gauge system, the ^{29}Si MAS NMR was implemented to fill in this knowledge gap. The ^{29}Si MAS NMR testing results revealed that the polymerization degree of the tetrahedral structure of $[SiO_4]$ increased when increasing the hydration time. The form of the [SiO4] was Si(Q2) and Si(Q3) in the amorphous C-A-S-H gel. In addition, the polymerization degree of tetrahedral [SiO4] and the amount of [AlO4] combined with [SiO4] in the hydration products reduced with an increase of the Ca/Si ratio [39].

Apart from the ^{27}Al and ^{29}Si NMR to investigate the structure of Al and Si, high-resolution transmission electron microscopy (HRTEM) was also used to observe the morphology and composition of the C-A-S-H gel. The HRTEM image indicated that the C-A-S-H phase was composed of a continuous amorphous phase and randomly distributed nanocrystalline with an average size of about 5 nm, shown in Figure 1. From a hydration model, it was claimed that the hydration process of the RM/coal gangue-based cementitious materials system can be divided into four types, including (1) the dissolution of the raw materials, (2) the formation of the C-A-S-H and AFt phases, (3) the condensation process to form hydration products, and (4) poly-condensation of the C-A-S-H phase. It was also stated that these four types of hydration processes occurred simultaneously with no strict time boundaries [40].

In addition to XRD, FTIR, SEM/EDS, and HRTEM, X-ray photoelectron spectroscopy (XPS) was also implemented to investigate the microstructure evolution process of the RM/coal gangue system. With a fixed RM to coal gangue mass ratio of 4:1, the Na/Al and Si/Al molar ratios were about 0.7 and 1:3, respectively. The results revealed that the binding energy of the Si 2p in the RM/coal gangue system was lower than the RM and coal gangue raw materials. After the alkali activation, the RM and coal gangue were both reacted and formed sodium aluminosilicate. The Si/O was decreased from 1/3.4 to 1/4.0. This phenomenon was considered as proof of the phase conversion of the crystallized structure to an amorphous structure. Meanwhile, the binding energy of the Al 2p was also lower in the RM/coal gangue system than the RM or coal gangue raw materials, due to the octahedral coordination in the cancrisilite or because the kaolinite had been transformed into a tetrahedral coordination [41].

Although the mechanical properties have been tested, and the microstructure evolution and the hydration products have been investigated, the durability of the RM/coal gange system has been barely reported on. The environmental resistance with exposure to freeze/thaw cycling, chemical attack, or heavy metals or toxic elements immobilization effects have not been systematically studied. In addition, despite the bonding condition of the Si, O, Ca, and Al being studied, the phase structure and chemical composition of the hydration products were not presented. Therefore, future studies should be focused on further microstructure evolution and the hydration mechanisms of the RM/coal gange system.

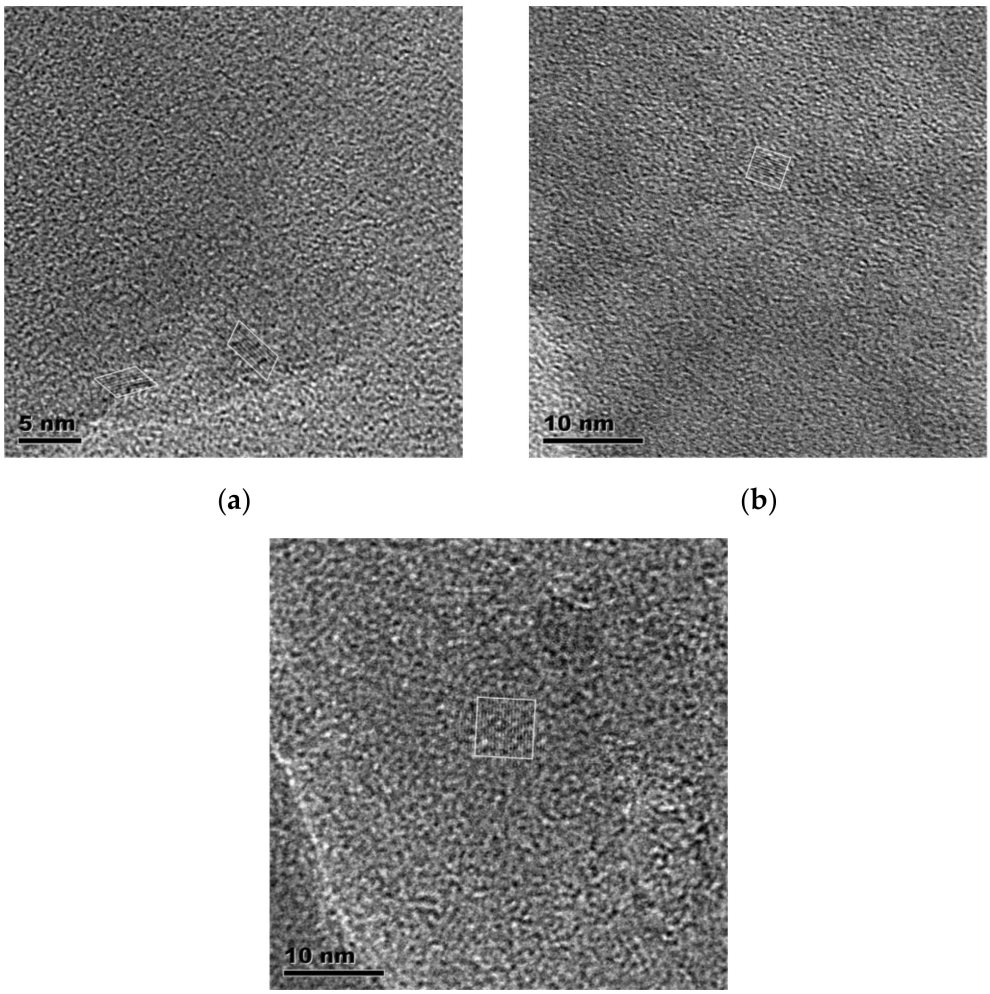

Figure 1. HRTEM images of the C-A-S-H phase in the 90 day RM/coal gangue paste with various Ca/Si ratios of (**a**) 0.95, (**b**) 1.04, and (**c**) 1.13 [40].

4. Metakaolin

Metakaolin is a typical aluminosilicate material that is originated from the calcination of clay and kaolinite, which is beneficial to enhance the pozzolanic reactivity as a resource for manufacturing cementitious materials. Prof. Joseph Davidovits has demonstrated that metakaolin plays a vital role in the formation of geopolymers. This statement has also been systematically investigated by Prof. Kriven et al. for decades [42]. As a result, it is feasible to manufacture a RM-based geopolymer by incorporating it with metakaolin.

The mechanical properties of RM/metakaolin geopolymers were investigated and the microstructures and potential hydration mechanism were investigated. It was found that the replacement of metakaolin by 25% of RM had no distinctive reduction of the compressive strength. The leaching test result indicated that the concentration of Na in the leachate was about 100 ppm. Although the RM provided the Al_2O_3, Fe_2O_3, and oxy-hydroxide, the XRD results demonstrated that the amorphous cementitious phase was about 90%. The authors also used SEM/EDS analysis to demonstrate the effect of Si/Al molar ratio on the mechanical properties and stated that the decrease of the SiO_2/Al_2O_3 ratio would reduce the mechanical properties of the RM/metakaolin geopolymer [43].

Despite the potential feasibility of RM/metakaolin-based cementitious materials that has been reported, it is not enough to elucidate the potential hydration mechanism by solely using XRD. Kaya further applied XRD along with FTIR and SEM to explore the

activation mechanism of the RM/metakaolin system. The highest content of RM was 40%, and the addition of RM increased the intensity of the XRD peaks of the aluminosilicate, hematite, and goethite phases. The main FTIR band form of the hydrated RM/metakaolin geopolymer was located at 989 cm^{-1}. Increasing the RM content resulted in a constant band shift to high frequencies, while the intensity of the main band reduced along with the broadening of the band [44].

By using FTIR technology, the effects of the Na/Al molar ratio on the mechanical properties and microstructure evolution process were explored. The results showed that the appropriate Na/Al molar ratio was beneficial to the geopolymerization process, but a high Na/Al molar ratio would destroy the microstructure of the geopolymers. The FTIR results, as shown in Figure 2, indicated that the primary band variation was located at 900–1200 cm^{-1} due to the asymmetric stretching vibration of a Si-O-R (R = Si or Al) bond, which is very similar to the RM/coal gangue system. In the RM/metakaolin sample, the peak at 1111 cm^{-1} was weaker than the RM raw material, suggesting an increase of the Al content in the aluminosilicates because of the replacement of the Al^{3+} to Si^{4+} in the silicon tetrahedron. This phenomenon revealed the bond breaking of the Si-O-R due to the dissolution and the occurrence of the geopolymer reaction. Meanwhile, the peak at 1093 cm^{-1} indicated the asymmetric stretching vibration of the Si-O-R bond, the absorption peak at 807 cm^{-1} corresponding to the asymmetric stretching vibration of the Al-O tetracoordinate bond, and the absorption peak at 468 cm^{-1} relating to the bending vibration of Si-O-Si and O-Si-O bonding. Furthermore, the CO_2 in the air reacted with the alkali and formed a small amount of Na_2CO_3; therefore, the peak intensities at 1410–1510 cm^{-1} and 879 cm^{-1}, which corresponded to the asymmetric stretching vibration of the O-C-O bond, increased with an increasing Na/Al ratio, suggesting a deeper reaction of alkali with CO_2 in the air and a higher degree of the polymerization process [45].

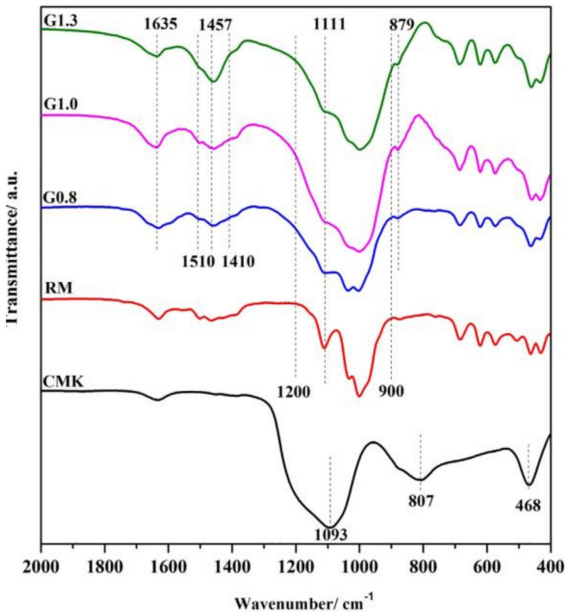

Figure 2. FTIR spectra of 28 d coal metakaolin (CMK), RM, and RM/CMK with a Na/Al ratio of 0.8 (G 0.8), 1.0 (G 1.0), and 1.3(G 1.3) in geopolymer [45].

In addition to the mechanical properties' investigation, the RM/metakaolin cementitious material was also investigated as a remediation of arsenic pollution. It was claimed that the RM/metakaolin system can be used as an eco-friendly and low-carbon cementitious material to alleviate the arsenic release from arsenic-containing sulfide minerals. It was found through QXRD results that arsenic could be effectively stabilized via the ion exchange in ettringite, Ca/Fe-As precipitation, and the encapsulation of the cementitious

hydration products. The leaching testing results indicated that the leaching concentration of arsenic in the 28 days geopolymer samples was slightly higher than the 7 days samples. The XPS results also demonstrated that the As(V) concentration was enhanced from about 10% to 20% after being cured for 28 days due to the formation of Fe-As and Ca-As compounds. In addition, the effect of the pH value on the arsenic leaching concentration was higher than the temperature, and a stable pH value was ranged from 2 to 5 [46].

Metakaolin-based geopolymer has been investigated for decades and the microstructure evolution, hydration products, and mechanical properties have been studied systematically; however, the durability of the metakaolin-based geopolymer is still the main challenge. The efflorescence problem and the alkali–silica reaction problems are still the primary shortcomings of the metakaolin-based geopolymer materials. How to immobilize the soluble ions and stabilize the alkali and heavy metal elements should be considered as the biggest challenge in future studies.

5. Slags

Although the synergistic use of RM/slag as an eco-friendly cementitious material has been investigated for decades, and the microstructure evolution, hydration process, and potential hydration product composition have been presented, agreement on the hydration process and mechanisms of this system is yet to be achieved. Steel slags or ground granular blast furnace slag (GGBS) is a type of granular powder material that is obtained from iron and steel-making. Previous studies have demonstrated that slag can be used as a good cementitious material due to its pozzolanic activity with high calcium and silicate contents [47–49]. Similar to other solid wastes, the chemical compositions of slags vary significantly depending on the origin of the steel ore. In general cases, the chemical compositions of slags are CaO (30–50%), SiO_2 (28–38%), Al_2O_3 (8–24%), and MgO (1–18%). Apart from the chemical composition, another important factor for the recycling of slag as cementitious materials is the reactivity of the raw materials. Slow cooling of slag will lead to high contents of unreactive crystalline Ca-Al-Mg silicates phases. As a result, the slag must be rapidly cooled or quenched below 800 °C to prevent the crystallization of the Ca-Al-Mg silicates phases.

In early 2000, the RM/slag system was introduced for cementitious materials. The alkali-activated RM/slag cementitious materials were prepared with a slag/RM mass ratio of 7:3. The microstructures were observed, and the potential hydration mechanisms were presented via XRD, TG/DTA, IR, and TEM/EDXA characterization. Although the authors did not clearly demonstrate the chemical compositions of the activators, and thus it is difficult to understand the hydration mechanism, the results can still provide some valuable information. The XRD results indicated that the hydration products were mainly composed of C-S-H gel with a low Ca/Si ratio. The content of the β-C_2S decreased with an increase of curing time and for the samples that were steam cured at 80 °C, no zeolite minerals were detected. The TEM/EDXA results claimed that the hydration products were amorphous C-S-H gels with a fibrous shape and dissolved with a small amount of Al_2O_3 and Fe_2O_3 [50].

The authors also investigated the mechanical properties and durability, including the resistance to carbonation, seawater, acid, sulfate, and freeze/thaw cycle attacks of this RM/slag system. The mechanical properties testing results indicated that the 1 d, 3 d, 28 d, and 180 d compressive strengths and bending strengths were 20.0, 28.1, 56.0, and 66.5 MPa, and 3.3, 4.9, 8.4, and 9.9 MPa, respectively. The durability testing results indicated that this RM/slag system had an outstanding chemical resistance performance and freeze/thaw resistance. The microstructure observation demonstrated that the hydration products were dense and integrated without crystallized products [51].

After decades of development, the RM/slag cementitious material has achieved considerable progress. Through aligning the moduli of water glass and curing condition, the optimized preparation condition of the RM/slag cementitious material was achieved by using a sodium silicate solution modulus of 2.0, with a RM to slag mass ratio of 1:1.

The 7 day compressive strength achieved 54 MPa at 25 °C. A novel hydration process characterization method was implemented by using the electric conductance curves of the fresh slurry of the RM/slag mixtures. The results demonstrated that the electric conductance curves of all samples were divided into two stages, as shown in Figure 3. At the early age of the hydration process, the ion concentrations were relatively high in the fresh paste because of the dissolution of the aluminosilicate material which contributed to the increase of the electrical conductance. With the extension of the reaction time, the electrical conductance decreased palpably due to the reduction of the mobile ions resulting from the geopolymerization process. This method briefly confirmed that the reaction stages of the RM/slag system without considering the water loss [52].

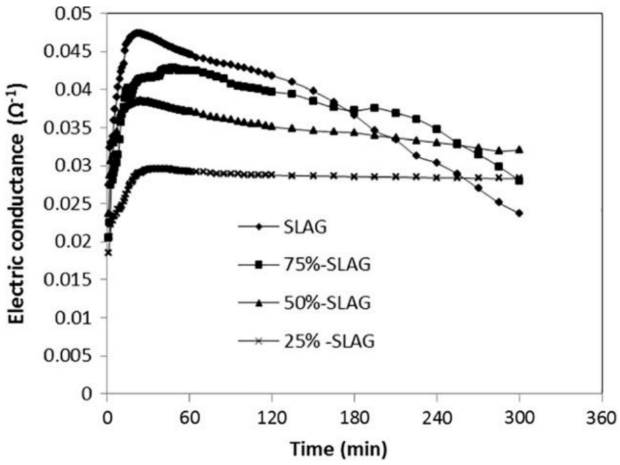

Figure 3. Electric conductance of geopolymers from slag and slag/RM prepared with sodium silicate solution of R = 2.0 [52].

Although the mechanical properties have been significantly improved in the past decades, the durability problem is still the biggest challenge of the RM/slag system. As a result, it is compelling to explore how to control the early age failure of this cementitious materials system. For the durability challenges, one of the most important failure types is efflorescence, which is a typical phenomenon of alkali-activated cementitious materials. In Kang's study, it was found that the efflorescence was governed by the diameter of the capillary pores. The acceleration of efflorescence was originated from the increase of the capillary pores with a diameter ranging from 10–1000 nm, and the moisture content was also a key factor that determined the efflorescence. The main chemical components of the efflorescence were sodium compounds including Na_2CO_3 and Na_2SO_4, due to the solution and precipitation along with the wet/dry cycles of the material [53]. Except for the sodium compounds, another study also found the existence of $CaCO_3$ in the leached salt through XRD characterization [54].

In concrete constructions with exposure to aggressive environments, the corrosion of the rebar resulting from chloride attack was the top challenge for the Portland cement concrete; however, it was found that the chloride penetration resistance in the RM/slag cementitious materials was much lower than in the ordinary Portland cement concrete. For the RM/slag mortar, when the content of chloride salt was lower than 0.5 wt% of the cementitious material, the average corrosion current of the steel bar was negligible. With the content of the chloride salt increased to over 0.5 wt%, the corrosion phenomenon started to become observable and was proportional to the content of the chloride, while the corrosion current of the steel bar was proportional to the chloride content. The critical chloride content was 0.3 wt.%, and the passivate degree of the geopolymer mortar was greater than the normal cement mortar [55].

Most recently, ultrafine RM powder was used to prepare an RM/slag cementitious material and its workability was investigated. In this contribution, the ultrafine RM powder

with 920 m^2/kg specific surface area was obtained by 900 mesh sieving after grinding. The microstructure was characterized by FTIR, XRD, MIP, and SEM/EDS analysis. It was found that the RM could extend the setting time and the hydration process of the ultrafine RM was faster than that of the coarse RM. Furthermore, the ultrafine RM was more beneficial to improve the slurry stability and mechanical properties than the coarse RM. The microstructure characterization results indicated that RM played a filling role in the geopolymerization process, and a reduction of the particle size could increase the reactivity of the RM. In addition, the iron components in ultrafine RM could also have participated in the geopolymerization process [56].

Similar to lime, which is beneficial for enhancing the early age mechanical properties, the conflict between the early age strength and workability of the RM/slag system is the primary challenge for practical applications. Furthermore, the hydration rates of the main chemical composition in slag and RM were not clear. The metastable hydration products, final hydration products, and the microstructure evolution process need to be determined. Chemical additives which fit this system should be developed to satisfy the requirements for practical applications.

6. Ashes

Coal fly ash, husk ash, or corn straw ash are all solid wastes composed of aluminosilicates. This chemical composition guarantees the potential feasibility of recycling them with RM to manufacture cementitious materials. The mechanical properties and microstructure of the RM/fly ash system were investigated and compared with metakaolin-based geopolymer materials. The results indicated that the metakaolin-based geopolymer had higher mechanical properties than the RM/fly ash geopolymer, and the metakaolin-based geopolymer had a shorter curing time than the RM/fly ash geopolymer because of the higher reactivity and smaller particle size of the metakaolin powder compared with that of the RM. The microstructure analysis demonstrated that the metakaolin-based geopolymer had some reprecipitated NaOH or Na_2CO_3 crystals, while some plate or needle-like shaped crystals were found in the pore space of the RM/fly ash system. The mechanical properties of the RM/fly ash geopolymer were not stable and were affected by multiple factors such as the origin of raw materials, concentration of activators, and curing conditions. In addition, this investigation suggested that the raw materials with a higher reactivity, higher Si/Al ratio, and higher concentration of alkali concentration can have a positive effect on the mechanical properties of the geopolymers [57].

The mechanical properties and microstructure evolution of the RM/fly ash system were affected by multiple factors, including curing temperature, curing time, and chemical compositions of the raw materials. It was found that the curing humidity had little effect on the improvement of mechanical properties. In addition, the compressive strength and the modulus increased with an increasing curing time. The XRD results indicated that the crystallized components in the raw materials were difficult to dissolve during the geopolymer process, and thus remained as filler in the final geopolymer products. The SEM/EDS analysis confirmed that the mechanical properties were governed by the Si/Al and Na/Al ratios. The nominal Na/Al molar ratio of 0.6–0.8 with the nominal Si/Al ratio of 2.0 was the optimized proportion for preparing geopolymers with various sources of raw materials [58]. Similar results were obtained by the investigation of XRD, FTIR, SEM, and TG, etc. [59–61].

Apart from the mechanical properties, the authors also investigated the durability and leaching behavior of heavy metals of the RM/fly ash system. With exposure to sulfuric acid of a pH value of 3.0, it was found that the compressive strength, flexural strength, and Young's modulus decreased by 30%, 70%, and 45%, respectively, compared with the control OPC samples. SEM, XRD, and FTIR results confirmed that the deterioration of mechanical properties was mainly originated from the dissolution of the amorphous binder phases. This dissolution process stopped after 7 days of soaking. The leaching testing results indicated that the concentrations of the As, Cu, Cr, and Cd in the leachate solution

of the RM/fly ash samples met the US EPA standard, and the leaching behavior of the heavy metals was independent of the curing temperature [62].

Except for the XRD, SEM, FTIR, or TG, Mid-Infrared spectroscopy (MIR) was used to detect the microstructure evolution of the RM/fly ash cementitious materials. Figure 4 gives the MIR spectroscopy results of the mixed raw materials and the 7 days RM/fly ash materials with fly ash contents of 0 wt.% (RFG-1), 14 wt.% (RFG-5), and 19 wt.% (RFG-7), respectively. As can be seen in this figure, in the MIR pattern of the raw materials, the absorption band at the 3610 cm^{-1}, which corresponds to the Ca-OH, was relatively strong due to the existence of the $Ca(OH)_2$ phase, while in the pattern of the RM/fly ash system, the intensity of the band at the 3610 cm^{-1} was relatively weak due to the occurrence of the pozzolanic reaction. Meanwhile, the absorption band at 3557 cm^{-1} corresponded to the stretching vibration of the Si-OH in the mixed raw materials. The 3416 cm^{-1} in the RM/fly ash system represented the octahedral structure of $[Al(OH)_6]^{3-}$ in the AFt phase. Quantitative calculation of the MIR results demonstrated that the integration degree of the sample with fly ash content of 14 wt.% was the strongest, suggesting the highest quantity of the $[Al(OH)_6]^{3-}$ phase contributed to the development of the mechanical properties. The band at 1626 cm^{-1} represented the bending vibration of H-O-H, the 874 cm^{-1} represented the asymmetric O-C-O, and the 1453 cm^{-1} represented the $CO_3{}^{-2}$ resulting from the carbonation of the materials [63].

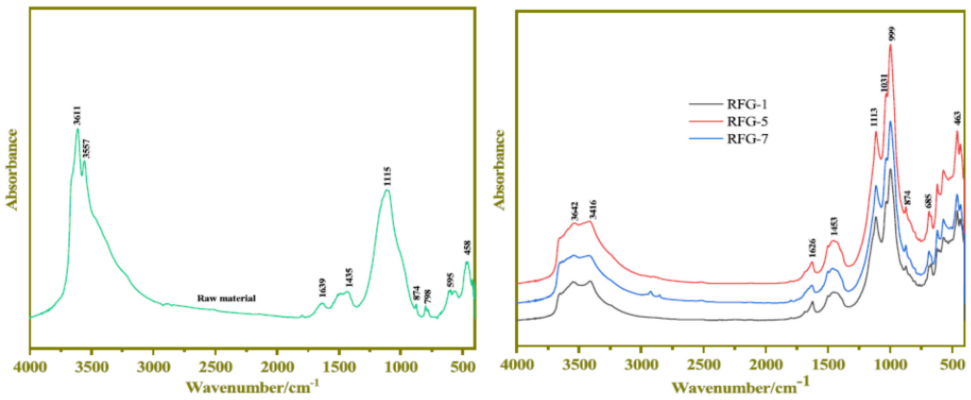

Figure 4. MIR spectra of mixed raw materials and samples with fly ash contents of 0 wt.% (RFG-1), 14 wt.% (RFG-5), and 19 wt.% (RFG-7) after 7 d hydration [63].

Excluding the fly ash, the rice husk ash is a giant branch of solid waste that is originates from agricultural production. The chemical contents of rice husk ash are similar to fly ash, which is mainly composed of aluminosilicate. As a result, it is feasible to utilize the rice husk ash and RM to manufacture eco-friendly cementitious materials. Recently, the mechanical properties of the RM/rice husk ash system were investigated. The results showed that the 28 days compressive strength can reach the range of 6.8 to 15.5 MPa [64]. The heavy metals leaching test results indicated that the RM/rice husk ash system could immobilize the leaching of the heavy metals, including Cu, Zn, Cd, Pb, Fe, and Cr, based on the European (EN 124572-2 EU CEN TC292/ CEN TC 308) standard with a pH value 7 [65]; however, the microstructure evolution and the hydration process were not investigated in these studies, which leaves a big opportunity for future studies.

7. Conclusions and Future Challenges

In summary, the recycling use of RM as eco-friendly cementitious materials along with other solid wastes is compelling from both academic and practical perspectives. Although the exploration for green and cost-effective cementitious materials has kept moving forwards, the current methodologies have shown their distinct shortcomings. In the manufacturing process, alkali-activation is still the main approach to realize the solidification of the RM solid waste systems. Although agreement of the formation of the binder phase real-

ized by a two-stage reaction process, namely, the dissolution and reprecipitation processes, has been achieved, the details of the hydration process and the reaction thermodynamics remain unclear. Previous studies observed that the hydration products are mainly composed of C-S-H, C-A-S-H, N-A-S-H, and M-A-S-H gels, and $Ca(OH)_2$, $Mg(OH)_2$, $CaCO_3$, AFt, AFm, and other crystals remaining from the raw materials. These microstructure characterizations were mostly analyzed through XRD, FTIR, MIR, DTA/TG, NMR, SEM, TEM, EDS, and XPS. The durability and heavy metals leaching properties were also investigated. The results indicated that the RM system has a great potential for manufacturing green cementitious materials. Table 1 lists the chemical composition, compressive strength, durability/heavy metals immobilization, microstructure characterization methods, and main hydration products reviewed in this article.

Table 1. Brief summary of synergistically using RM and other solid wastes to manufacture cementitious materials.

Materials	Chemical Compositions	Compressive Strength	Durability, Heavy Metals Immobilization	Microstructure Characterization Methods	Hydration Products
Lime	CaO/MgO 5–10%	15–18 Mpa (28 d) [26]; 11.2 MPa (365 d) [27];	Stabilization of Pb, Cd, and Zn [30–32]; Cu, Pb, and Zn [34];	XRD, DTG, and SEM [26]; XRD and SEM [27]; XRD and SEM/EDS [28]; SEM and TGA [34];	$CaCO_3$ and Ca^{2+} compounds [25]; stratlingite (C_2ASH_8) and carbonates [26]; $Ca_3Al_2O_6$, c-AlO(OH), FeO(OH), C-S-H and $CaAl_2Si_2O_8{\cdot}4H_2O$ [28]; calcium sulfoferrite hydration products [33]
Coal gangue	SiO_2 (52–65%), Al_2O_3 (16–36%), Fe_2O_3 (2.28–14.63%), K_2O/Na_2O (1.45–3.9%), CaO (0.42–2.32%), MgO (0.44–2.41%), TiO_2 (0.90–4%), and P_2O_5 (0.007~0.24%)	1–7 MPa [37];	/	SEM [35]; XRD, FTIR, and TG/DTA [36–38]; XPS [41]	ettringite, C-S-H and N-A-S-H [35]; aluminous C-S-H, C-A-S-H and $Ca_3Al_2O_6{\cdot}xH_2O$ [36]; AFt [40];
Metakaolin	SiO_2 (50–60%), Al_2O_3 (30–40%), Fe_2O_3 (1–2%), CaO (0.2%), and TiO_2 (2%)	55 MPa (28 d) [45]	/	SEM/EDS [43]; SEM, XRD, FTIR [44]; XPS [46];	N-A-S-H and C-A-S-H [42–46]
Slag	CaO (30–50%), SiO_2 (28–38%), Al_2O_3 (8–24%), and MgO (1–18%)	67 MPa (28 d) [51]; 54 (7 d) MPa [52];	Na_2CO_3 and Na_2SO_4 (efflorescence compounds) [53]	XRD, TG/DTA, IR, and TEM/EDXA [50]; FTIR, XRD, MIP, and SEM/EDS [56]	C-S-H [50];
Ashes	SiO_2 (15–60%), Al_2O_3 (5–35%), Fe_2O_3 (4–40%), and CaO (1–40%)	16 MPa (28 d) [64]	As, Cu, Cr, and Cd [63], Cu, Zn, Cd, Pb, Fe, and Cr [65]	XRD, FTIR, SEM, and TG [59–61]; SEM, XRD, Mid-Infrared spectroscopy (MIR), FTIR [62]; XRD, SEM, FTIR, or TG [63];	$Ca(OH)_2$, octahedral structure of $[Al(OH)_6]^{3-}$ in the AFt [63]

As can be seen from Table 1, the hydration mechanisms of the RM-based cementitious materials with diverse solid wastes remain unclear. To further improve the mechanical properties, durability, and environmental stability, and to demonstrate the hydration

process and hydration products, further researches must be focused on the following perspectives in the next steps:

1. Solving the conflict between the early age strength development and the workability of the alkali-activated RM system.
2. Expanding the types of other solid wastes, such as corn straw ash, demolished concrete waste, and sludges.
3. Exploration of the durability of the RM system when exposed to an aggressive environment, including moisture environment, freeze/thaw cycling, acid attacks, and chloride and sulfate attacks, needs to be expanded.
4. The efflorescence problem and the ASR problems are still the natural shortcomings of the alkali-activated cementitious materials.
5. Microstructure analysis was limited to XRD, SEM, FTIR, and TG. The deep analysis of the HRTEM, NMR, XPS is quite limited.
6. The simulation work of the microstructure evolution process is still lacking.

Author Contributions: L.F. prepared the majority of this manuscript; W.Y. and N.C. oversaw the outline arrangement; K.Z. mainly contributed to the discussion and revision; and N.X. oversaw the whole contents. All authors have read and agreed to the published version of the manuscript.

Funding: This research was funded by the National Natural Science Foundation of China (Project Nos. 51772128 and 51632003), Youth Innovation Support Program of Shandong Colleges and Universities, Taishan Scholar Program, Case-by-Case Project for Top Outstanding Talents of Jinan, Double Hundred Foreign Expert Program (WST2018011), and Lianyungang Gaoxin District International Scientific Cooperation Program (HZ201902), Sino-European Research Center program (SERC-M-20191201), and Lianyungang Haiyan Plan program (2019-QD-002).

Institutional Review Board Statement: Not applicable.

Informed Consent Statement: Not applicable.

Data Availability Statement: The data presented in this study are available in Web of Science, Google Scholar, and Scopus.

Acknowledgments: We appreciate the discussion from Pengkun Hou, Jiabin Li, and Jing Zhong for their valuable suggestions.

Conflicts of Interest: The authors declare no conflict of interest.

References

1. Wang, S.; Jin, H.; Deng, Y.; Xiao, Y. Comprehensive utilization status of red mud in China: A critical review. *J. Clean. Prod.* **2021**, *289*, 125136. [CrossRef]
2. Dentoni, V.; Grosso, B.; Pinna, F. Experimental Evaluation of PM Emission from Red Mud Basins Exposed to Wind Erosion. *Minerals* **2021**, *11*, 405. [CrossRef]
3. Deady, É.A.; Evangelos, M.; Kathryn, G.; Ben, J.W.; Frances, W. A review of the poten-tial for rare-earth element resources from European red muds: Examples from Seydişehir, Turkey and Parnassus-Giona, Greece. *Mineral. Mag.* **2016**, *80*, 43–61. [CrossRef]
4. Wang, M.; Liu, X. Applications of red mud as an environmental remediation material: A review. *J. Hazard. Mater.* **2020**, *408*, 124420. [CrossRef] [PubMed]
5. Schmitz, C. (Ed.) *Handbook of Aluminium Recycling*; Vulkan-Verlag GmbH: Essen, Germany, 2006.
6. Ortega, J.M.; Cabeza, M.; Tenza-Abril, A.J.; Real-Herraiz, T.; Climent, M.Á.; Sánchez, I. Effects of red mud addition in the microstructure, durability and mechanical performance of cement mortars. *Appl. Sci.* **2019**, *9*, 984. [CrossRef]
7. Davidovits, J. *Geopolymer Chemistry and Applications*; Geopolymer Institute: Saint-Quentin, France, 2008. Available online: www.geopolymer.org (accessed on 12 May 2021).
8. Glukhovsky, V.D. Ancient, modern and future concretes. In Proceedings of the First International Conference on Alkaline Cements and Concretes, Kiev, Ukraine, 11–14 October 1994; pp. 1–9.
9. Granizo, M.L.; Blanco, M.T. Alkaline activation of metakaolin an isothermal conduction calorimetry study. *J. Therm. Anal. Calorim.* **1998**, *52*, 957–965. [CrossRef]
10. Granizo, M.L.; Alonso, S.; Blanco-Varela, M.T.; Palomo, A. Alkaline Activation of Metakaolin: Effect of Calcium Hydroxide in the Products of Reaction. *J. Am. Ceram. Soc.* **2004**, *85*, 225–231. [CrossRef]
11. Bocullo, V.L.; Vitola, D.; Kantautas, A.; Bajare, D. The influence of the SiO2/Na2O ratio on the low calci-um alkali activated binder based on fly ash. *Mater. Chem. Phys.* **2021**, *258*, 123846. [CrossRef]

12. Singh, P.S.; Trigg, M.; Burgar, I.; Bastow, T. Geopolymer formation processes at room temperature studied by 29Si and 27Al MAS-NMR. *Mater. Sci. Eng. A* **2005**, *396*, 392–402. [CrossRef]
13. Zhang, W.; Liu, X.; Wang, Y.; Li, Z.; Li, Y.; Ren, Y. Binary reaction behaviors of red mud based cementitious material: Hydration characteristics and Na+ utilization. *J. Hazard. Mater.* **2020**, *410*, 124592. [CrossRef]
14. Pontikes, Y.; Angelopoulos, G. Bauxite residue in cement and cementitious applications: Current status and a possible way forward. Resour. *Conserv. Recycl.* **2013**, *73*, 53–63. [CrossRef]
15. Pontikes, Y.; Angelopoulos, G.; Blanpain, B. Radioactive elements in Bayer's process bauxite residue and their impact in valorization options. In Proceedings of the EAN NORM Workshop, Leuven, Belgium, 29 November–1 December 2011.
16. Biswas, W.K.; Cooling, D. Sustainability Assessment of Red Sand as a Substitute for Virgin Sand and Crushed Limestone. *J. Ind. Ecol.* **2013**, *17*, 756–762. [CrossRef]
17. Technology Roadmap. *Maximising the Use of Bauxite Residue in Cement*; International Aluminium Institute: London, UK, 2020. Available online: https://international-aluminium.org/resource/technology-roadmap-maximizing-the-use-of-bauxite-residue-in-cement/ (accessed on 15 November 2020).
18. Rabl, A.; Joseph, V.; Zoughaib, A. Environmental impacts and costs of solid waste: A comparison of land-fill and incineration. *Waste Manag. Res.* **2008**, *26*, 147–162. [CrossRef] [PubMed]
19. Bélanger, M.-J. Red mud stacking. In *Essential Readings in Light Metals*; Springer: Cham, Switzerland, 2016; pp. 944–950.
20. Luo, Z.; Lam, S.K.; Hu, S.; Chen, D. From generation to treatment: A systematic reactive nitrogen flow assessment of solid waste in China. *J. Clean. Prod.* **2020**, *259*, 121127. [CrossRef]
21. Khairul, M.A.; Zanganeh, J.; Moghtaderi, B. The composition, recycling and utilisation of Bayer red mud. Resources. *Conserv. Recycl.* **2019**, *141*, 483–498. [CrossRef]
22. Liu, X.; Zhang, N. Utilization of red mud in cement production: A review. *Waste Manag. Res.* **2011**, *29*, 1053–1063. [CrossRef]
23. Mukiza, E.; Zhang, L.; Liu, X.; Zhang, N. Utilization of red mud in road base and subgrade materi-als: A review. *Resour. Conserv. Recycl.* **2019**, *141*, 87–199. [CrossRef]
24. Paramguru, R.K.; Rath, P.C.; Misra, V.N. Trends in red mud utilization—A review. *Miner. Process. Extr. Metall. Rev.* **2004**, *26*, 1–29. [CrossRef]
25. Arjun, D.; Malhotra, S.K. Lime-stabilized red mud bricks. *Mater. Struct.* **1990**, *23*, 252–255.
26. Gordon, J.; Willard, N.; Pinnock, R.; Marcia, M. A preliminary investigation of strength development in Ja-maican red mud composites. *Cem. Concr. Compos.* **1996**, *18*, 371–379. [CrossRef]
27. Mymrin, V.; Alekseev, K.; Fortini, O.M.; Aibuldinov, Y.K.; Pedroso, C.L.; Nagalli, A.; Costa, E.B. Environmentally clean materials from hazardous red mud, ground cooled ferrous slag and lime production waste. *J. Clean. Prod.* **2017**, *161*, 376–381. [CrossRef]
28. Liu, S.; Li, Z.; Li, Y.; Cao, W. Strength properties of Bayer red mud stabilized by lime-fly ash using orthogonal experiments. *Constr. Build. Mater.* **2018**, *166*, 554–563. [CrossRef]
29. Kumar, S.; Prasad, A. Parameters controlling strength of red mud-lime mix. *Eur. J. Environ. Civ. Eng.* **2019**, *23*, 743–757. [CrossRef]
30. Garau, G.; Castaldi, P.; Santona, L.; Deiana, P.; Melis, P. Influence of red mud, zeolite and lime on heavy metal immobilization, culturable heterotrophic microbial populations and enzyme activities in a contaminated soil. *Geoderma* **2007**, *142*, 47–57. [CrossRef]
31. Friesl, W.; Lombi, E.; Horak, O.; Wenzel, W.W. Immobilization of heavy metals in soils using inor-ganic amendments in a greenhouse study. *J. Plant Nutr. Soil Sci.* **2003**, *166*, 191–196. [CrossRef]
32. Gray, C.; Dunham, S.; Dennis, P.; Zhao, F.; McGrath, S. Field evaluation of in situ remediation of a heavy metal contaminated soil using lime and red-mud. *Environ. Pollut.* **2006**, *142*, 530–539. [CrossRef]
33. Li, Y.-C.; Min, X.-B.; Ke, Y.; Chai, L.-Y.; Shi, M.-Q.; Tang, C.-J.; Wang, Q.-W.; Liang, Y.-J.; Lei, J.; Liu, D.-G. Utilization of red mud and Pb/Zn smelter waste for the synthesis of a red mud-based cementitious material. *J. Hazard. Mater.* **2018**, *344*, 343–349. [CrossRef]
34. Wang, F.; Pan, H.; Xu, J. Evaluation of red mud based binder for the immobilization of copper, lead and zinc. *Environ. Pollut.* **2020**, *263*, 114416. [CrossRef]
35. Zhang, N.; Sun, H.; Liu, X.; Zhang, J. Early-age characteristics of red mud–coal gangue cementitious material. *J. Hazard. Mater.* **2009**, *167*, 927–932. [CrossRef]
36. Zhang, N.; Liu, X.; Sun, H.; Li, L. Pozzolanic behaviour of compound-activated red mud-coal gangue mixture. *Cem. Concr. Res.* **2011**, *41*, 270–278. [CrossRef]
37. Koshy, N.; Kunga, D.; Liming, H.; Qingbo, W.; Jay, N.M. Synthesis and characterization of geopol-ymers derived from coal gangue, fly ash and red mud. *Constr. Build. Mater.* **2019**, *206*, 287–296. [CrossRef]
38. Chen, S.; Du, Z.; Zhang, Z.; Yin, D.; Feng, F.; Ma, J. Effects of red mud additions on gangue-cemented paste backfill properties. *Powder Technol.* **2020**, *367*, 833–840. [CrossRef]
39. Liu, X.; Zhang, N.; Yao, Y.; Sun, H.; Feng, H. Micro-structural characterization of the hydration products of bauxite-calcination-method red mud-coal gangue based cementitious materials. *J. Hazard. Mater.* **2013**, *262*, 428–438. [CrossRef] [PubMed]
40. Zhang, N.; Li, H.; Liu, X. Hydration mechanism and leaching behavior of bauxite-calcination-method red mud-coal gangue based cementitious materials. *J. Hazard. Mater.* **2016**, *314*, 172–180. [CrossRef] [PubMed]
41. Geng, J.; Zhou, M.; Zhang, T.; Wang, W.; Wang, T.; Zhou, X.; Wang, X.; Hou, H. Preparation of blended geopolymer from red mud and coal gangue with mechanical co-grinding preactivation. *Mater. Struct.* **2016**, *50*, 109. [CrossRef]

42. Xie, N.; Bell, J.L.; Kriven, W.M. Fabrication of Structural Leucite Glass-Ceramics from Potassium-Based Geopolymer Precursors. *J. Am. Ceram. Soc.* **2010**, *93*, 2644–2649. [CrossRef]
43. Hajjaji, W.S.; Andrejkovičová, C.; Zanelli, M.; Alshaaer, M.; Dondi, J.A.; Rocha, F. Composition and techno-logical properties of geopolymers based on metakaolin and red mud. *Mater. Des.* **2013**, *52*, 648–654. [CrossRef]
44. Kaya, K.; Soyer-Uzun, S. Evolution of structural characteristics and compressive strength in red mud–metakaolin based geopolymer systems. *Ceram. Int.* **2016**, *42*, 7406–7413. [CrossRef]
45. Liu, J.; Li, X.; Lu, Y.; Bai, X. Effects of Na/Al ratio on mechanical properties and microstructure of red mud-coal metakaolin geopolymer. *Constr. Build. Mater.* **2020**, *263*, 120653. [CrossRef]
46. Zhou, X.; Zhang, Z.-F.; Yang, H.; Bao, C.-J.; Wang, J.-S.; Sun, Y.-H.; Liu, D.-W.; Shen, P.-L.; Su, C. Red mud-metakaolin based cementitious material for remediation of arsenic pollution: Stabilization mechanism and leaching behavior of arsenic in lollingite. *J. Environ. Manag.* **2021**, *300*, 113715. [CrossRef]
47. Ortega, J.M.; Esteban, M.D.; Sánchez, I.; Climent, M. Performance of Sustainable Fly Ash and Slag Cement Mortars Exposed to Simulated and Real In Situ Mediterranean Conditions along 90 Warm Season Days. *Materials* **2017**, *10*, 1254. [CrossRef] [PubMed]
48. Zhang, J.; Tan, H.; Bao, M.; Liu, X.; Luo, Z.; Wang, P. Low carbon cementitious materi-als: Sodium sulfate activated ultra-fine slag/fly ash blends at ambient temperature. *J. Clean. Prod.* **2021**, *280*, 124363. [CrossRef]
49. Zhang, J.; Tan, H.; He, X.; Yang, W.; Deng, X. Utilization of carbide slag-granulated blast fur-nace slag system by wet grinding as low carbon cementitious materials. *Constr. Build. Mater.* **2020**, *249*, 118763. [CrossRef]
50. Pan, Z.; Cheng, L.; Lu, Y.; Yang, N. Hydration products of alkali-activated slag–red mud cementitious material. *Cem. Concr. Res.* **2002**, *32*, 357–362. [CrossRef]
51. Pan, Z.; Li, D.; Yu, J.; Yang, N. Properties and microstructure of the hardened alkali-activated red mud–slag cementitious material. *Cem. Concr. Res.* **2003**, *33*, 1437–1441. [CrossRef]
52. Lemougna, P.N.; Wang, K.-T.; Tang, Q.; Cui, X. Study on the development of inorganic polymers from red mud and slag system: Application in mortar and lightweight materials. *Constr. Build. Mater.* **2017**, *156*, 486–495. [CrossRef]
53. Kang, S.-P.; Kwon, S. Effects of red mud and alkali-activated slag cement on efflorescence in cement mor-tar. *Constr. Build. Mater.* **2017**, *133*, 459–467. [CrossRef]
54. Hyeok-Jung, K.; Suk-Pyo, K.; Gyeong-Cheol, C. Effect of red mud content on strength and efflorescence in pavement using alkali-activated slag cement. *Int. J. Concr. Struct. Mater.* **2018**, *12*, 1–9. [CrossRef]
55. Liang, X.; Ji, Y. Experimental study on durability of red mud-blast furnace slag geopolymer mortar. *Constr. Build. Mater.* **2020**, *267*, 120942. [CrossRef]
56. Li, Z.; You, H.; Gao, Y.; Wang, C.; Zhang, J. Effect of ultrafine red mud on the workability and micro-structure of blast furnace slag-red mud based geopolymeric grouts. *Powder Technol.* **2021**, *392*, 610–618. [CrossRef]
57. He, J.; Zhang, J.; Yu, Y.; Zhang, G. The strength and microstructure of two geopolymers derived from metakaolin and red mud-fly ash admixture: A comparative study. *Constr. Build. Mater.* **2012**, *30*, 80–91. [CrossRef]
58. Zhang, M.; Tahar, E.-K.; Zhang, G.; Liang, J.; Tao, M. Synthesis factors affecting mechanical properties, microstructure, and chemical composition of red mud–fly ash based geopolymers. *Fuel* **2014**, *134*, 315–325. [CrossRef]
59. Koshy, N.; Dondrob, K.; Hu, L.; Wen, Q.; Meegoda, J.N. Mechanical Properties of Geopolymers Synthesized from Fly Ash and Red Mud under Ambient Conditions. *Crystals* **2019**, *9*, 572. [CrossRef]
60. Wei, H.; Nie, Q.; Huang, B.; Shu, X.; He, Q. Mechanical and microstructural characterization of geo-polymers derived from red mud and fly ashes. *J. Clean. Prod.* **2018**, *186*, 799–806.
61. Li, Y.; Min, X.; Ke, Y.; Liu, D.; Tang, C. Preparation of red mud-based geopolymer mate-rials from MSWI fly ash and red mud by mechanical activation. *Waste Manag.* **2019**, *83*, 202–208. [CrossRef] [PubMed]
62. Zhang, M.; Zhao, M.; Zhang, G.; Mann, D.; Lumsden, K.; Tao, M. Durability of red mud-fly ash based geopolymer and leaching behavior of heavy metals in sulfuric acid solutions and deionized water. *Constr. Build. Mater.* **2016**, *124*, 373–382. [CrossRef]
63. Li, Y.; Liu, X.; Li, Z.; Ren, Y.; Wang, Y.; Zhang, W. Preparation, characterization and application of red mud, fly ash and desulfurized gypsum based eco-friendly road base materials. *J. Clean. Prod.* **2020**, *284*, 124777. [CrossRef]
64. Thang, N.H.; Nhung, L.T.; Quyen, P.V.T.H.; Phong, D.T.; Khe, D.T.; Van Phuc, N. Development of heat resistant geopolymer-based materials from red mud and rice husk ash. *AIP Conf. Proc.* **2018**, *1954*, 040005. [CrossRef]
65. Nguyen, H.T.; Pham, V.T.H.Q.; Dang, T.P.; Dao, T.K. Leachability of heavy metals in geopolymer-based materials synthesized from red mud and rice husk ash. *AIP Conf. Proc.* **2018**, *1954*, 040014. [CrossRef]